



# Global Biogeochemical Cycles

## RESEARCH ARTICLE

10.1002/2013GB004760

Yonghui Wang and Huiying Liu contributed equally to this work.

### Key Points:

- Four year continuous hourly monitoring of soil CO<sub>2</sub> flux ( $R_s$ ) using automated system
- Non-growing-season cumulative  $R_s$  accounted for 11.8–13.2% of the annual total  $R_s$
- Higher  $Q_{10}$  of thawed than frozen soil can trigger C loss in warmer winter

### Supporting Information:

- Readme
- Table S1
- Table S2
- Table S3
- Figure S1
- Figure S2
- Figure S3
- Figure S4
- Figure S5

### Correspondence to:

J.-S. He,  
jshe@pku.edu.cn

### Citation:

Wang, Y., et al. (2014), Non-growing-season soil respiration is controlled by freezing and thawing processes in the summer monsoon-dominated Tibetan alpine grassland, *Global Biogeochem. Cycles*, 28, 1081–1095, doi:10.1002/2013GB004760.

Received 31 OCT 2013

Accepted 10 SEP 2014

Accepted article online 12 SEP 2014

Published online 10 OCT 2014

## Non-growing-season soil respiration is controlled by freezing and thawing processes in the summer monsoon-dominated Tibetan alpine grassland

Yonghui Wang<sup>1</sup>, Huiying Liu<sup>1</sup>, Haegeun Chung<sup>2</sup>, Lingfei Yu<sup>3</sup>, Zhaorong Mi<sup>4</sup>, Yan Geng<sup>1</sup>, Xin Jing<sup>1</sup>, Shiping Wang<sup>5</sup>, Hui Zeng<sup>6</sup>, Guangmin Cao<sup>4</sup>, Xinquan Zhao<sup>4</sup>, and Jin-Sheng He<sup>1,4</sup>

<sup>1</sup>Department of Ecology, College of Urban and Environmental Sciences, and Key Laboratory for Earth Surface Processes of the Ministry of Education, Peking University, Beijing, China, <sup>2</sup>Department of Environmental Engineering, Konkuk University, Seoul, South Korea, <sup>3</sup>State Key Laboratory of Vegetation and Environmental Change, Institute of Botany, Chinese Academy of Sciences, Beijing, China, <sup>4</sup>Key Laboratory of Adaptation and Evolution of Plateau Biota, Northwest Institute of Plateau Biology, Chinese Academy of Sciences, Xining, China, <sup>5</sup>Key Laboratory of Tibetan Environment Changes and Land Surface Processes, Institute of Tibetan Plateau Research, Chinese Academy of Sciences, Beijing, China, <sup>6</sup>Key Laboratory for Urban Habitat Environmental Science and Technology, Peking University Shenzhen Graduate School, Shenzhen, China

**Abstract** The Tibetan alpine grasslands, sharing many features with arctic tundra ecosystems, have a unique non-growing-season climate that is usually dry and without persistent snow cover. Pronounced winter warming recently observed in this ecosystem may significantly alter the non-growing-season carbon cycle processes such as soil respiration ( $R_s$ ), but detailed measurements to assess the patterns, drivers of, and potential feedbacks on  $R_s$  have not been made yet. We conducted a 4 year study on  $R_s$  using a unique  $R_s$  measuring system, composed of an automated soil CO<sub>2</sub> flux sampling system and a custom-made container, to facilitate measurements in this extreme environment. We found that in the nongrowing season, (1) cumulative  $R_s$  was 82–89 g C m<sup>-2</sup>, accounting for 11.8–13.2% of the annual total  $R_s$ ; (2) surface soil freezing controlled the diurnal pattern of  $R_s$  and bulk soil freezing induced lower reference respiration rate ( $R_0$ ) and temperature sensitivity ( $Q_{10}$ ) than those in the growing season (0.40–0.53 versus 0.84–1.32  $\mu\text{mol CO}_2 \text{ m}^{-2} \text{ s}^{-1}$  for  $R_0$  and 2.5–2.9 versus 2.9–5.6 for  $Q_{10}$ ); and (3) the intraannual variation in cumulative  $R_s$  was controlled by accumulated surface soil temperature. We found that in the summer monsoon-dominated Tibetan alpine grassland, surface soil freezing, bulk soil freezing, and accumulated surface soil temperature are the day-, season-, and year-scale drivers of the non-growing-season  $R_s$ , respectively. Our results suggest that warmer winters can trigger carbon loss from this ecosystem because of higher  $Q_{10}$  of thawed than frozen soils.

## 1. Introduction

Non-growing-season soil respiration ( $R_s$ ) is an essential component of the global carbon cycling [Fahnestock et al., 1998; Monson et al., 2006a], and thus, it is crucial to thoroughly understand how it feedbacks to climate change [Belshe et al., 2013; Brooks et al., 2004; Campbell et al., 2005]. Alpine and arctic tundra ecosystems are vulnerable and sensitive to climate change because of their large soil carbon storage, high soil carbon density [McGuire et al., 2009; Yang et al., 2008], and vast area of permafrost [Koven et al., 2011]. In these ecosystems, the decomposition of soil organic carbon during the nongrowing season can occur at a high rate [Monson et al., 2006b] due to soil microbes that maintain their activities at extremely low temperature [Panikov et al., 2006]. Thus, the non-growing-season  $R_s$  can contribute significantly to annual carbon budgets [Liptzin et al., 2009]. For instance, in heath tundra ecosystems, non-growing-season cumulative  $R_s$  ranges from 103 to 176 g C m<sup>-2</sup>, accounting for 14–40% of the annual total  $R_s$  [Elberling, 2007; Larsen et al., 2007; Morgner et al., 2010]. In sedge and tussock tundra ecosystems, non-growing-season cumulative  $R_s$  ranges from 10 to 68 g C m<sup>-2</sup>, contributing to 17–30% of the annual total  $R_s$  [Fahnestock et al., 1999; Morgner et al., 2010; Oechel et al., 1997; Sullivan et al., 2008; Welker et al., 2004]. Grogan and Chapin [1999] used soda lime to measure respiration in acidic tussock tundra in Alaska and reported an extremely large value, 189 g C m<sup>-2</sup>, contributing up to 52% of the annual total  $R_s$ .

The drivers of the day-, season-, and year-scale variations of the non-growing-season  $R_s$  have been shown to be different from those of the growing-season  $R_s$ . On the day scale, both distinct [Elberling and Brandt, 2003;

Kato et al., 2004; Seok et al., 2009] and indistinct diurnal patterns [Mariko et al., 2000; Mo et al., 2005; Zimov et al., 1996] have been observed. However, the drivers of the non-growing-season diurnal patterns of  $R_s$  have not been studied sufficiently, and only in one study in heath tundra of northeastern Greenland, it has been reported that the diurnal pattern of  $R_s$  during fast soil thawing period was partly influenced by soil thawing [Elberling and Brandt, 2003]. On the season scale, non-growing-season  $R_s$  is primarily due to microbial decomposition of soil organic carbon and tends to have a higher-temperature sensitivity ( $Q_{10}$ ) than the growing-season  $R_s$ . This higher  $Q_{10}$  can be due to either fast substrate utilization of the unique soil microbial communities in snow-covered soils [McMahon et al., 2011; Monson et al., 2006b] or indirect controls of temperature on diffusion of extracellular enzymes and substrates through effects on physical factors [Mikan et al., 2002]. Finally, on the year scale, the interannual variation of the non-growing-season cumulative  $R_s$  has been found to be regulated by snow depth in seasonal snow-covered ecosystems [Monson et al., 2006b; Nobrega and Grogan, 2007]. These studies indicate that the non-growing-season  $R_s$  is sensitive to changes in climate, especially the temperature, and the duration and depth of snow cover, highlighting the importance of systematic investigation of the non-growing-season  $R_s$ .

The Tibetan alpine grassland is as vulnerable and sensitive to climate warming as the arctic tundra and may release a large amount of  $\text{CO}_2$  to atmosphere when facing rising temperature [Belshe et al., 2013; Koven et al., 2011; McGuire et al., 2009; Tan et al., 2010; Xu et al., 2010]. Alpine grassland of the Tibetan Plateau and arctic tundra share many similar features, such as a long nongrowing season, large soil carbon storage, high carbon density [McGuire et al., 2009; Shi et al., 2012; Yang et al., 2008], and large area of permafrost [Cheng, 2005; Cheng and Wu, 2007; Dörfer et al., 2013; Koven et al., 2011]. Recent studies have shown that the Tibetan Plateau acts as a carbon sink, e.g., the net ecosystem  $\text{CO}_2$  exchanges of alpine shrubland ecosystem and alpine meadow ecosystem were  $\sim -70 \text{ g C m}^{-2} \text{ yr}^{-1}$  (ranged from  $-58.5$  to  $-75.5 \text{ g C m}^{-2} \text{ yr}^{-1}$ ) and  $\sim -120.9 \text{ g C m}^{-2} \text{ yr}^{-1}$  (ranged from  $-78.5$  to  $-192.5 \text{ g C m}^{-2} \text{ yr}^{-1}$ ), respectively [Kato et al., 2006; Zhao et al., 2006]. Our previous study has reported that across the grasslands of the plateau, peak growing-season soil respiration is well predicted by belowground biomass and soil moisture, but not soil temperature [Geng et al., 2012], highlighting the need to further explore the effect of soil temperature. In addition, further investigations have reported that the mean  $R_s$  of the northeastern part of the plateau is  $0.96 \mu\text{mol CO}_2 \text{ m}^{-2} \text{ s}^{-1}$  ( $1 \text{ g C m}^{-2} \text{ d}^{-1}$ ) between December and February [Cao et al., 2004], and the mean non-growing-season  $R_s$  is  $0.74 \mu\text{mol CO}_2 \text{ m}^{-2} \text{ s}^{-1}$  in a cropland ecosystem located in the southern part of the plateau [Shi et al., 2006], indicating a large non-growing-season cumulative  $R_s$  ( $140\text{--}180 \text{ g C m}^{-2}$ ) on this plateau. These data suggest that carbon loss on this plateau during the nongrowing season cannot be overlooked, emphasizing its important role in global carbon cycling.

The climate of the Tibetan Plateau is unique in comparison with other alpine and tundra ecosystems, because it is dominated by a monsoon. Specifically, in winter, the plateau is a source of cool air, with a higher atmosphere pressure than the surrounding areas. Therefore, the atmosphere current flows out of the plateau, and the climate is usually cold and dry. In summer, this plateau is a source of warm air with a lower atmosphere pressure than the surroundings, and thus the moist air moves toward the plateau, which creates a warm and humid climate [Tang and Reiter, 1984]. The nongrowing season of this plateau receives  $< 15\%$  of the annual precipitation and thus has no persistent snowpack [Tian et al., 2003; Zhang et al., 1995], in contrast to other tundra and alpine ecosystems where the nongrowing season receives  $50\text{--}80\%$  of the annual precipitation, and the depth of snowpack is usually  $> 100 \text{ cm}$  [Brooks et al., 2004; Liptzin et al., 2009; Morgner et al., 2010]. Thorough understanding of the patterns of and drivers for non-growing-season  $R_s$  and evaluating its potential feedbacks to climate warming in Tibetan alpine grassland are urgently needed as the permafrost area in this ecosystem has been shrinking during the past several decades due to rapid increases in annual and winter temperature [Cheng and Wu, 2007; Piao et al., 2010; Wu and Zhang, 2010; You et al., 2010; Zhang et al., 2013]. Although the importance of the non-growing-season  $R_s$  of the Tibetan alpine grassland has been recognized [Cao et al., 2004; Shi et al., 2006], the low time resolution (once per month) and short-term (1–2 years) measurements of previous studies, along with the complex relationships between drivers of non-growing-season  $R_s$ , limit our ability to accurately model its trend and potential responses to climate warming.

We conducted a 4 year study on  $R_s$  in alpine grasslands of the Tibetan Plateau. This is the first attempt to measure hourly  $R_s$  and heterotrophic respiration ( $R_h$ ) throughout the year in a long-term experiment, made possible by

**Table 1.** Climate Characteristics of the Study Site<sup>a</sup>

	2009	2010	2011	2012
<i>Overall</i>				
Annual mean air temperature (°C)	−0.81 (−23.60 – 14.20)	−0.83 (−22.58 – 17.31)	−1.46 (−23.38 – 14.63)	−1.82 (−21.96 – 14.34)
Annual mean ST <sub>0</sub> (°C)	4.25 (−15.66 – 17.48)	4.07 (−15.74 – 22.71)	2.48 (−18.02 – 20.40)	3.37 (−23.92 – 23.14)
Annual mean ST <sub>5</sub> (°C)	2.81 (−10.16 – 15.62)	2.38 (−8.50 – 16.92)	1.79 (−11.35 – 13.61)	1.12 (−10.65 – 13.77)
Annual precipitation (mm)	350.6	480.8	501.3	367.3
<i>Nongrowing Season</i>				
Length (day)	175	193	182	189
Mean air temperature (°C)	−8.97 (−23.60 – 1.42)	−8.19 (−22.58 – 2.40)	−9.47 (−23.38 – 3.08)	−9.81 (−21.96 – 1.96)
Mean ST <sub>0</sub> (°C)	−4.62 (−15.66 – 7.99)	−4.76 (−15.74 – 7.38)	−5.61 (−18.02 – 5.99)	−4.58 (−23.92 – 7.34)
Mean ST <sub>5</sub> (°C)	−3.58 (−10.16 – 5.12)	−3.35 (−8.50 – 4.46)	−4.03 (−11.35 – 5.33)	−4.15 (−10.65 – 3.50)
Precipitation (snowfall, mm)	19.4	34.5	39.9	27.4
Number of days with surface soil freezing (day)	142	170	158	154
Number of days with daily maximum ST <sub>0</sub> > 0°C (day)	170	184	172	163
Number of days of snow recorded (day)	30	21	20	34
<i>Growing Season</i>				
Length (day)	190	172	183	177
Mean air temperature (°C)	6.70 (−2.93 – 14.20)	7.43 (−4.03 – 17.31)	6.51 (−2.70 – 14.63)	6.71 (−1.54 – 14.34)
Mean ST <sub>0</sub> (°C)	12.28 (4.79 – 17.48)	13.84 (4.06 – 22.71)	11.29 (4.60 – 20.40)	11.85 (2.03 – 23.14)
Mean ST <sub>5</sub> (°C)	8.70 (−0.11 – 15.62)	8.82 (0.10 – 16.92)	7.57 (−0.97 – 13.61)	7.45 (−0.23 – 13.77)
Precipitation (rainfall, mm)	331.2	446.3	461.4	339.9

<sup>a</sup>ST<sub>0</sub>: surface soil temperature; ST<sub>5</sub>: soil temperature at 5 cm depth. Values in brackets are the ranges of the daily mean temperature.

employing a unique  $R_s$  measurement system. More specifically, a custom-made container, which maintained the internal temperature above 5°C, was used to protect our instruments from the extremely low temperature of the nongrowing season. During the nongrowing season in the Tibetan Plateau, the bulk soil is usually frozen, while the daily range of surface soil temperature is large and the daily maximum surface soil temperature is usually > 0°C due to the absence of persistent snowpack. Therefore, we first hypothesized that on the Tibetan Plateau, the non-growing-season cumulative  $R_s$  is large but its annual contribution is lower than those in the seasonal snow-covered ecosystems due to the lack of insulation by snowpack. We also hypothesized that the day-, season-, and year-scale processes of the non-growing-season  $R_s$  are driven by the daily surface soil freezing-thawing process (surface soil freezing), the seasonal change of bulk soil frozen-thawed condition (bulk soil freezing), and the accumulated soil temperature, respectively.

## 2. Materials and Methods

### 2.1. Study Site

Our study site is at the HaiBei Alpine Grassland Ecosystem Research Station (HaiBei Station, 101°12'E, 37°30'N, 3200 m above sea level), located in the northeastern part of the Tibetan Plateau, China. This area, dominated by alpine grassland, has a continental monsoon climate, with a long nongrowing season and a short growing season [Zhao and Zhou, 1999]. From 2009 to 2012, the mean annual air temperature ranged from −0.81 to −1.82°C and the annual precipitation from 350.6 to 501.3 mm (Table 1). Generally, the nongrowing season starts in late October and ends in mid-April. Though the nongrowing season is as long as 180 days, it receives only 6–8% of the annual precipitation; this period is usually characterized as dry, cold, and with no persistent snowpack (Table 1). The soil developed is Mat-Gryic Cambisol [Chinese Soil Taxonomy Research Group, 1995]. Soil organic carbon content and bulk density at 0–10 cm and 10–20 cm depth were 63 and 36 g kg<sup>−1</sup> soil and 0.82 and 0.98 g cm<sup>−3</sup>, respectively (L. Lin, unpublished data, 2013). The pH value of the 0–10 cm soil was 6.4 [Jing et al., 2013].

The plant community is dominated by *Kobresia humilis*, *Festuca ovina*, *Elymus nutans*, *Poa pratensis*, *Carex scabrirostris*, *Scripus distigmaticus*, *Gentiana straminea*, *Gentiana farreri*, *Leontopodium odiumnum*, *Blvsus sinocompressus*, *Potentilla nivea*, and *Dasiphora fruticosa*, and the aboveground net primary production was about 350 g m<sup>−2</sup> yr<sup>−1</sup> (300–450 g m<sup>−2</sup> yr<sup>−1</sup>) from 2006 to 2010 [Wang et al., 2012]. Detailed information on our study site and the experimental platform can be found in previously published papers [Kimball et al., 2008; Luo et al., 2010].

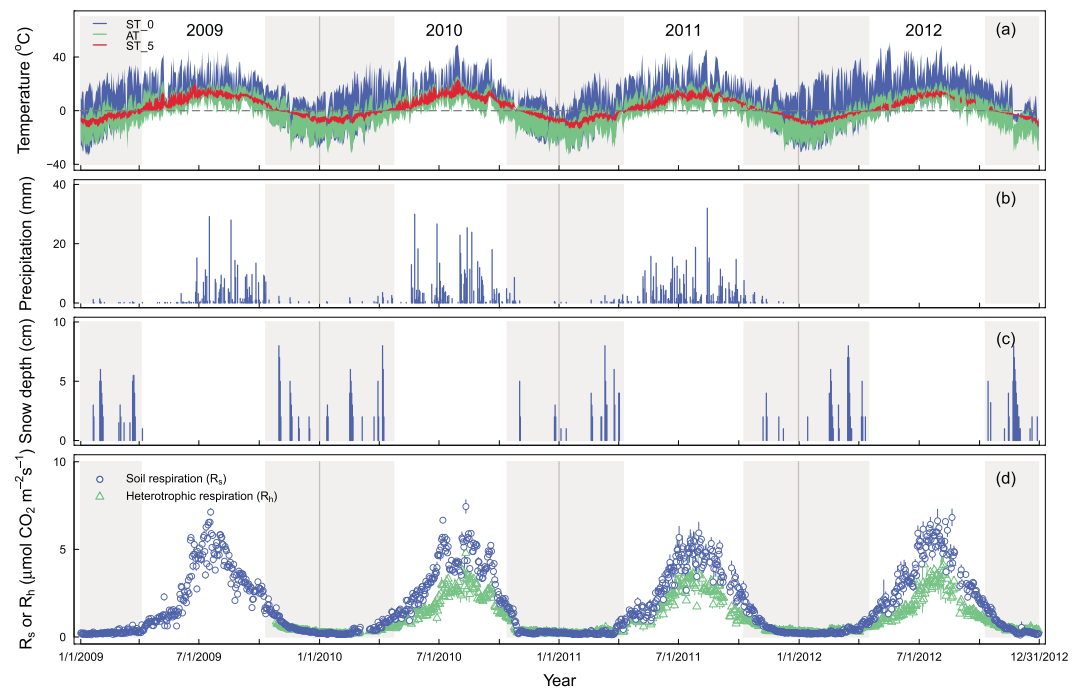


**Figure 1.** Seasonal and annual variation of (a) air temperature (AT), surface soil temperature (ST\_0), and soil temperature at 5 cm depth (ST\_5); (b) precipitation; (c) snow depth; and (d) soil respiration rate ( $R_s$ ) and heterotrophic respiration rate ( $R_h$ ). Shading periods represent the nongrowing season. Vertical bars represent the standard error of the means ( $n = 3\text{--}4$  for  $R_s$  and  $n = 2$  for  $R_h$ ).

## 2.2. Measurements of Soil Respiration, Heterotrophic Respiration, Air Temperature, and Soil Temperature

A square study site (27 m side length) was separated into four rows of 3 m width. Each row was then further separated into four 3 m diameter circular areas (3 m interval), and one of them was randomly selected as sampling plot; thus, there were four plots to measure  $R_s$  and  $R_h$  (Figure S1 in the supporting information). In each plot, a polyvinyl chloride collar (20 cm diameter and 10 cm height) was installed to a soil depth of 3 cm and a deep collar (20 cm diameter and 65 cm height) was installed to a soil depth of 60 cm to exclude plant roots and organic matter inputs (> 90% of the belowground biomass is distributed in the top 20 cm of soil). The shallow and deep collars were used to measure  $R_s$  and  $R_h$ , respectively. The effect of dead roots on  $R_h$  was large in the first growing season after the insertion of deep collar, but it subsided in the following year (Figure S2). To avoid the effects of dead roots on  $R_h$ , only the  $R_h$  data from January 2010 to December 2012 were included in our analyses.

We had four replicates (from January to October 2009) or three replicates (from November 2009 to December 2012) for  $R_s$  and two replicates for  $R_h$  (from October 2009 to December 2012) for the hourly data (Figure 1) automatically measured using the LI-8150 Multiplexer composed of a LI-8100 Automated Soil CO<sub>2</sub> Flux System and five LI-8100-104 long-term chambers (Li-Cor Inc., Lincoln, NE, USA). As the non-growing-season temperature is extremely low, the instruments were placed in a custom-made container (60 cm long, 70 cm wide, and 70 cm high; power by AC220V) to protect them from extremely low temperature and ensure their normal operation. The internal temperature of this container was controlled by a heating system composed of a Toky-AI208 temperature controller (Toky Electrical Co., Ltd., Zhongshan, Guangdong, China), a temperature sensor, and heating cable embedded in the internal surface of the container. The heating system maintained the internal temperature of the container above 5°C.

We also added one more replicate for  $R_s$  and two more replicates for  $R_h$ , measured manually at an interval of 5–7 days using the LI-8100 Automated Soil CO<sub>2</sub> Flux System with LI-8100-103 short-term chamber from November 2009 to the end of 2012. The manual measurements were carried out at different plots but at the same time as the measurements of automated CO<sub>2</sub> analyzer. The means of manually measured  $R_s$  (or  $R_h$ ) and those of automatically measured  $R_s$  (or  $R_h$ ) were calculated separately. Subsequently, the slopes of

regression line between these two groups of means were compared to a 1:1 line using standardized major axis estimation in the R package *smatr* [R Core Team, 2012]. The slopes did not differ significantly from 1 ( $P > 0.05$ , Figure S3), indicating that our plots selected adequately sampled the extant spatial variation. Thus, although only the hourly data from long-term measurements (three to four replicates for  $R_s$  and two replicates for  $R_h$ ) were used to investigate the day-, season-, and year-scale variations of the non-growing-season  $R_s$  (or  $R_h$ ), our results should be reliable.

Data on soil temperature and moisture at 5 cm depth (ST\_5 and SM\_5) were automatically collected at an interval of 1 h through Decagon EC-5 Soil Moisture Sensors (Decagon Devices Inc., Pullman, WA, USA) and LI-8150-203 soil temperature probes attached to long-term chambers. We also collected hourly data on air temperature (AT) and bare-surface soil temperature (ST\_0), as well as daily precipitation (rainfall and snowfall) from a weather station located near our study site (< 50 m).

### 2.3. Definition of the Nongrowing Season, the Surface Soil Freezing, and the Bulk Soil Freezing

The definition of the nongrowing season in this study follows that of previous phenological studies [Körner and Paulsen, 2004; Piao et al., 2007; Tanja et al., 2003], meta-analysis of winter ecosystem respiration [Wang et al., 2011], and carbon flux research in boreal black spruce forest of Canada [Bergeron et al., 2007]. The first day that the 7 day smoothed daily mean AT remained  $< 0^\circ\text{C}$  for at least five consecutive days was defined as the start of the nongrowing season. Similarly, the first day that the 7 day smoothed daily mean AT remained  $> 0^\circ\text{C}$  for at least five consecutive days was defined as the onset of the growing season.

In the nongrowing season, the daily maximum ST\_0 was frequently higher than  $0^\circ\text{C}$  (Figure 1), although the bulk soil was frozen. Surface soil freezing and bulk soil freezing are different and should not be confused. The former occurs at the day scale, regulating daily variation; the latter occurs at the season scale and regulates seasonal variation. Thus, referenced to Konestabo et al. [2007] and Zhu et al. [2012], a day was identified as having a surface soil freezing when it matched the following conditions: (1) daily minimum ST\_0 below  $0^\circ\text{C}$  for at least 3 h and (2) daily maximum ST\_0 above  $0^\circ\text{C}$  for at least 3 h. The definition of bulk soil freezing was based on the 7 day smoothed daily minimum or maximum ST\_5 (ST\_5<sub>min</sub> or ST\_5<sub>max</sub>). Bulk soil is considered thawed when daily ST\_5<sub>min</sub> remains  $> 0^\circ\text{C}$  for at least five consecutive days; it is considered frozen when daily ST\_5<sub>max</sub> remains  $< 0^\circ\text{C}$  for at least five consecutive days [Guo et al., 2011].

### 2.4. Statistical Analysis

The hourly  $R_s$  and  $R_h$  rates were used to calculate the daily mean respiration rates, seasonal mean respiration rates, cumulative respiration, contribution of the non-growing-season  $R_s$  to annual total  $R_s$ , and the contribution of seasonal variation in  $R_h$  to  $R_s$ . Nonlinear regression approach with a four-parameter Gaussian function was employed to investigate the seasonal variations in diurnal patterns of  $R_s$ , because this function performed better than the quadratic function, sinusoidal function, and three-parameter Gaussian function (Table S1). This function is as follows:

$$R_{s,\text{Hour}} = a + b \times e^{\left[-0.5 \times \left(\frac{\text{BST}_{\text{hour}} - c}{d}\right)^2\right]} \quad (1)$$

where  $R_{s,\text{Hour}}$  is the simulated hourly  $R_s$  rate and  $\text{BST}_{\text{hour}}$  is the Beijing Standard Time (BST, UTC + 08). The parameters  $a$ ,  $b$ ,  $c$ , and  $d$  represent four characteristics of the diurnal curve:  $a$ , the daily minimum  $R_s$  rate;  $b$ , the amplitude;  $c$ , the time  $R_s$  rate reaches its peak value; and  $d$ , the width of peak (Figure 3a). The paired samples  $t$  test was used to identify the differences of parameters between the nongrowing season and the growing season.

The  $Q_{10}$  function was employed in investigating the dependence of  $R_s$  (or  $R_h$ ) on temperature as follows:

$$\ln R_{s,\text{Day}} = m + n \times T \quad \text{or} \quad R_{s,\text{Day}} = e^m \times e^{n \times T} \quad (2)$$

where  $\ln R_{s,\text{Day}}$  or  $R_{s,\text{Day}}$  are natural-log-transformed daily mean respiration rate ( $\ln R_{s,\text{Day}}$  or  $\ln R_{h,\text{Day}}$ ) or daily mean respiration rate ( $R_s$  or  $R_h$ ) and  $T$  is the daily mean temperature. In this study, the natural-log-transformed respiration rate was used, as it can clearly display the seasonal variation of temperature dependence of  $R_s$  [Elberling and Brandt, 2003; Tilston et al., 2010]. Parameters  $m$  and  $n$ , representing

**Table 2.** The Non-Growing-Season and the Growing-Season Mean Soil Respiration ( $R_s$ ) Rate ( $1 \mu\text{mol CO}_2 \text{ m}^{-2} \text{ s}^{-1} = 12 \mu\text{g C m}^{-2} \text{ s}^{-1}$ ), Contribution of Heterotrophic Respiration ( $R_h$ ), the Ratio of Non-Growing-Season  $R_h$  to the Growing-Season  $R_h$  ( $\text{NG\_}R_h/\text{GS\_}R_h$ ), Cumulative  $R_s$ , and the Contribution of Non-Growing-Season  $R_s$  to Annual Total  $R_s^a$

	2009	2010	2011	2012
<i>Mean <math>R_s</math> Rate</i>				
Nongrowing season ( $\mu\text{mol CO}_2 \text{ m}^{-2} \text{ s}^{-1}$ )	0.49 (0.02)	0.44 (0.02)	0.43 (0.07)	0.45 (0.06)
Growing season ( $\mu\text{mol CO}_2 \text{ m}^{-2} \text{ s}^{-1}$ )	2.97 (0.04)	3.41 (0.06)	3.22 (0.27)	3.45 (0.26)
<i>Contribution of <math>R_h</math></i>				
Nongrowing season (%)	—	91.8 (9.1)	98.1 (11.9)	88.1 (4.2)
Growing season (%)	—	58.5 (0.7)	59.6 (4.5)	51.2 (5.0)
$\text{NG\_}R_h/\text{GS\_}R_h$ (%)	—	22.4 (0.9)	22.1 (0.8)	23.9 (0.3)
<i>Cumulative <math>R_s</math></i>				
Nongrowing season ( $\text{g C m}^{-2}$ )	89 (4)	87 (5)	82 (13)	88 (12)
Growing season ( $\text{g C m}^{-2}$ )	584 (9)	609 (10)	612 (51)	633 (48)
Non-growing-season contribution (%)	13.2 (0.5)	12.5 (0.4)	11.8 (1.1)	12.2 (0.9)

<sup>a</sup>Values in brackets are the standard error of the means ( $n = 3-4$  for  $R_s$  and  $n = 2$  for  $R_h$ ).

intercept and slope, respectively, were used to calculate the reference respiration rate ( $R_0$ , simulated  $R_s$  rate at  $0^\circ\text{C}$ ) and temperature sensitivity ( $Q_{10}$ ) with the following functions:

$$R_0 = e^m \tag{3}$$

$$Q_{10} = e^{(10 \times n)} \tag{4}$$

A large body of work has shown that enzyme-catalyzed reactions can occur below  $0^\circ\text{C}$  [Monson et al., 2006b; Panikov et al., 2006], while in frozen soil, extremely slow diffusion of extracellular enzymes and substrates and/or intracellular desiccation can significantly influence temperature dependence of  $R_s$  [Davidson and Janssens, 2006; Mikan et al., 2002]. Thus, piecewise linear regression (PLR) was used to explore whether there is a breakpoint in the functional relationship between respiration and temperature. In this analysis, the breakpoint was defined as the temperature where the residual standard error of the PLR model reached its minimum value. The ordinary linear regression (OLR) and PLR models were compared using an  $F$  test. Only when the PLR model performed better than the OLR model was the breakpoint considered significant [Toms and Lesperance, 2003]. The intercept and slope parameters were employed to calculate the  $R_0$  and  $Q_{10}$  before and after the breakpoint using equations (3) and (4). Analysis of covariance (ANCOVA) was conducted to investigate the difference of  $R_0$  (or  $Q_{10}$ ) between the nongrowing season and the growing season.

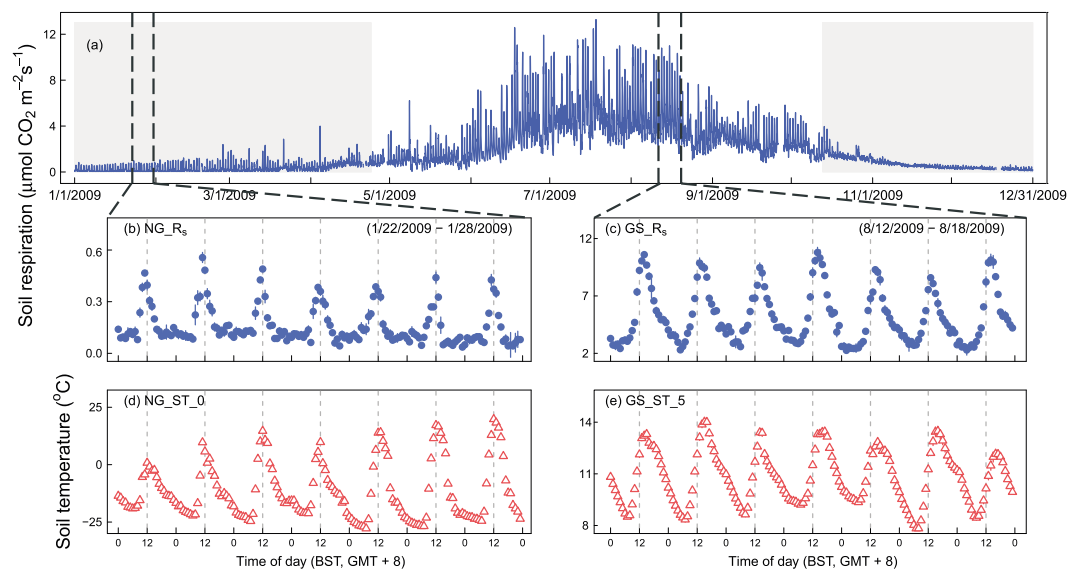


**Figure 2.** Comparisons of (a) diurnal patterns of (b) the non-growing-season soil respiration ( $\text{NG\_}R_s$ ), (c) the growing-season soil respiration ( $\text{GS\_}R_s$ ), (d) the non-growing-season surface soil temperature ( $\text{NG\_ST\_0}$ ), and (e) the growing-season soil temperature at 5 cm depth ( $\text{GS\_ST\_5}$ ). Vertical bars represent the standard error of the means ( $n = 3-4$ ).

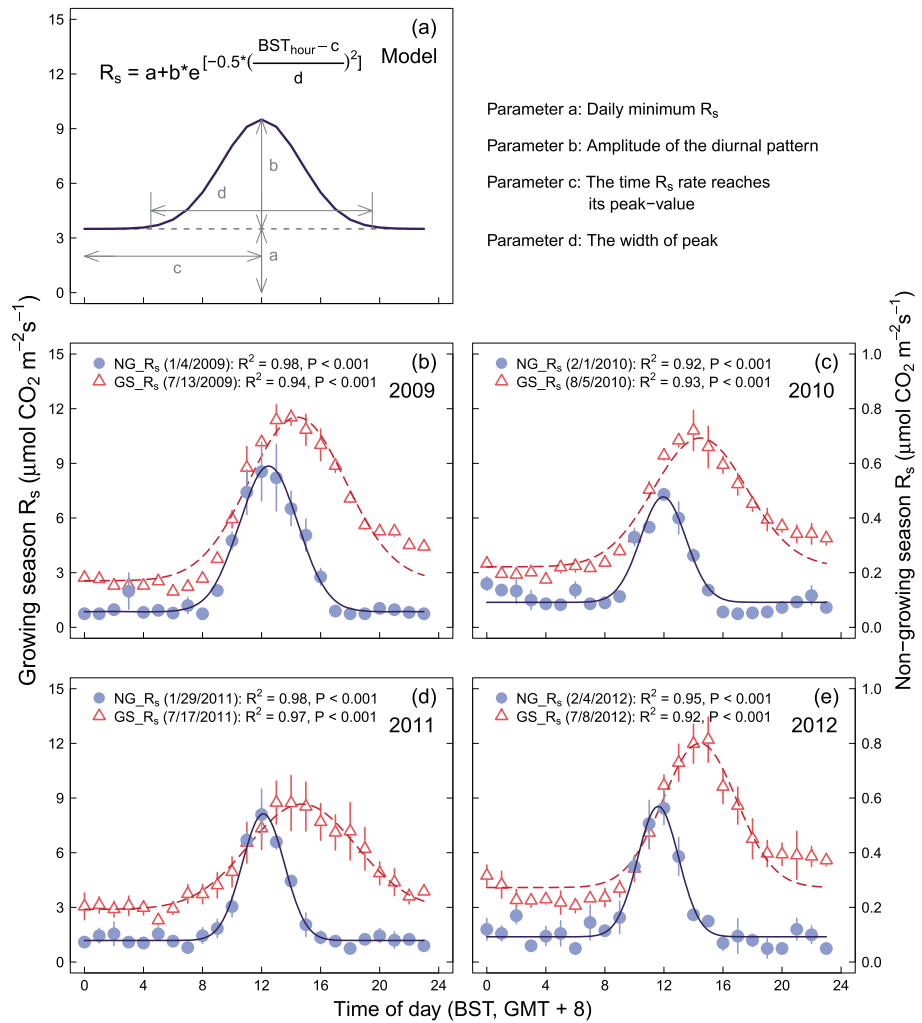


**Figure 3.** Comparisons of observed and simulated  $R_s$  diurnal patterns. (a) The four-parameter Gaussian function. (b–e) Observed (triangles and circles) and simulated (dashed and solid lines)  $R_s$  diurnal patterns of the nongrowing season (NG\_ $R_s$ ) and the growing season (GS\_ $R_s$ ). Vertical bars represent the standard error of the means ( $n = 3–4$ ).

The  $Q_{10}$  function was also used to determine the functional relationship between the daily cumulative  $R_s$  and the daily accumulated  $ST_0$  ( $ST_0 > 0^\circ\text{C}$ ) in the nongrowing season. Here the daily accumulated  $ST_0$  was calculated based on hourly  $ST_0$  data and defined as the sum of  $ST_0$  when it is higher than  $0^\circ\text{C}$ . The daily cumulative  $R_s$  is the sum of hourly measured  $R_s$ , which was averaged across replicated collars ( $n = 3–4$ ).

All statistical analyses were performed, and graphs were prepared using R 2.15.1 software [R Core Team, 2012]. Differences were considered to be significant when the  $P$  value was  $\leq 0.05$ .

### 3. Results

#### 3.1. Climate Characteristics of the Study Site

From 2009 to 2012, the non-growing-season precipitation varied from 19.4 to 39.9 mm, contributing to only 6–8% of the annual total. There was no persistent snowpack in the nongrowing seasons; the number of days of snow recorded was only 20–34 days. The number of daily maximum  $ST_0$  higher than  $0^\circ\text{C}$  was 163–184 days, and the number of days with surface soil freezing was 142–170 days in the nongrowing seasons (Figure 1 and Table 1).

#### 3.2. Quantity and Source of the Non-Growing-Season $R_s$

From 2009 to 2012,  $R_s$  showed a clear seasonal pattern, with averages of  $0.43–0.49 \mu\text{mol CO}_2 \text{ m}^{-2} \text{ s}^{-1}$  in the nongrowing season and  $2.97–3.45 \mu\text{mol CO}_2 \text{ m}^{-2} \text{ s}^{-1}$  in the growing season (Figure 1 and Table 2).

**Table 3.** Comparisons of Diurnal Pattern Parameters Between the Nongrowing Season and the Growing Season<sup>a</sup>

	2009	2010	2011	2012
<i>Daily Minimum R<sub>s</sub> (Parameter a)</i>				
Nongrowing season	0.36 (0.03) b	0.36 (0.02) b	0.38 (0.06) b	0.26 (0.03) b
Growing season	2.16 (0.02) a	2.62 (0.03) a	2.49 (0.17) a	2.67 (0.15) a
<i>Amplitude of the Diurnal Pattern (Parameter b)</i>				
Nongrowing season	0.50 (0.05) b	0.29 (0.05) b	0.24 (0.06) b	0.20 (0.03) b
Growing season	2.82 (0.06) a	2.63 (0.17) a	2.77 (0.38) a	3.08 (0.33) a
<i>The Time R<sub>s</sub> Rate Reaches Its Peak Value (Parameter c)</i>				
Nongrowing season	12.48 (0.21) b	13.33 (0.27) a	12.98 (0.17) b	12.65 (0.20) b
Growing season	14.23 (0.14) a	14.11 (0.07) a	13.94 (0.15) a	14.06 (0.10) a
<i>The Width of Peak (Parameter d)</i>				
Nongrowing season	2.03 (0.11) b	2.62 (0.31) a	1.99 (0.10) b	2.46 (0.30) a
Growing season	2.79 (0.05) a	2.91 (0.09) a	2.61 (0.04) a	2.43 (0.05) a

<sup>a</sup>Values in brackets are the standard error of the means ( $n = 3-4$ ). Letters (a and b) within a column represent significant difference between parameters (paired  $t$  test,  $P < 0.05$ ).

The non-growing-season cumulative  $R_s$  ranged from 82 to 89 g C m<sup>-2</sup>, contributing to 11.8–13.2% of the annual cumulative  $R_s$  (Table 2). The interannual variation of both the non-growing-season cumulative  $R_s$  (coefficient of variation (CV) = 3.6% across 4 years) and its contribution to annual total  $R_s$  (CV = 5.5% across 4 years) was small.  $R_h$  was the major component of  $R_s$ , contributing to 88.1–98.1% of the non-growing-season  $R_s$  and 51.2–59.6% of the growing-season  $R_s$  (Table 2). The soil organic carbon decomposed in the nongrowing season was 22.1–23.9% of that during the growing season (Table 2).

### 3.3. Diurnal Pattern of $R_s$ in the Non-Growing-Season

Across the 4 years,  $R_s$  displayed clear diurnal patterns (Figures 2a–2c), and the four-parameter Gaussian function explained > 90% of its variation (Figures 3b–3e). Further analysis showed that the daily minimum  $R_s$  rates (parameter  $a$ ) and amplitudes (parameter  $b$ ) of the non-growing-season diurnal curves were significantly lower than their growing-season counterparts (paired  $t$  test,  $P < 0.05$ , Table 3), and the diurnal curves of the nongrowing season had significantly earlier peaks than those of the growing season (paired  $t$  test,  $P < 0.05$ , Table 3), although this trend was not significant in 2010 (paired  $t$  test,  $P > 0.05$ , Table 3).

The peak time of  $R_s$  diurnal pattern was consistent with that of ST\_0 in the nongrowing season (Figures 2b and 2d), while in the growing season, it had a similar peak time with that of ST\_5 (Figures 2c and 2e). The explanatory power of ST\_0 and ST\_5 in predicting the  $R_s$  in the nongrowing and the growing seasons was compared. In the nongrowing season, the explanatory power of ST\_0 (13.1–25.2%) was equal to or larger than that of ST\_5 (9.8–26.0%, Table 4). In the growing season, however, ST\_5 (66.5–80.9%) was a better predictor of  $R_s$  than ST\_0 (35.2–53.8%, Table 4).

### 3.4. Temperature Dependence of $R_s$ and $R_h$ in the Non-Growing-Season

The PLR approach demonstrated that a breakpoint around 0°C exists in the functional relationship between  $\ln R_{s,Day}$  and ST\_5 (Figure 4). Given that the freezing point of water is 0°C (neglecting salinity effects), 0°C was

**Table 4.** Correlations Between Soil Respiration ( $R_s$ ) and Soil Temperature During the Nongrowing Season and the Growing Season<sup>a</sup>

	2009	2010	2011	2012
<i>Nongrowing Season (Frozen Soil)</i>				
$R_s$ versus ST_0	0.224 (0.079) a	0.131 (0.003) a	0.252 (0.070) a	0.200 (0.053) a
$R_s$ versus ST_5	0.165 (0.095) b	0.098 (0.008) b	0.260 (0.120) a	0.189 (0.103) a
<i>Growing Season (Thawed Soil)</i>				
$R_s$ versus ST_0	0.352 (0.038) b	0.359 (0.029) b	0.526 (0.040) b	0.538 (0.041) b
$R_s$ versus ST_5	0.666 (0.034) a	0.724 (0.030) a	0.809 (0.019) a	0.665 (0.037) a

<sup>a</sup>Values in brackets are the standard error of the means ( $n = 3-4$ ). Letters (a and b) within a column represent significant difference between explanation powers ( $R^2$ ) of surface soil temperature (ST\_0) and soil temperature at 5 cm depth (ST\_5) on  $R_s$  (paired  $t$  test,  $P < 0.05$ ).

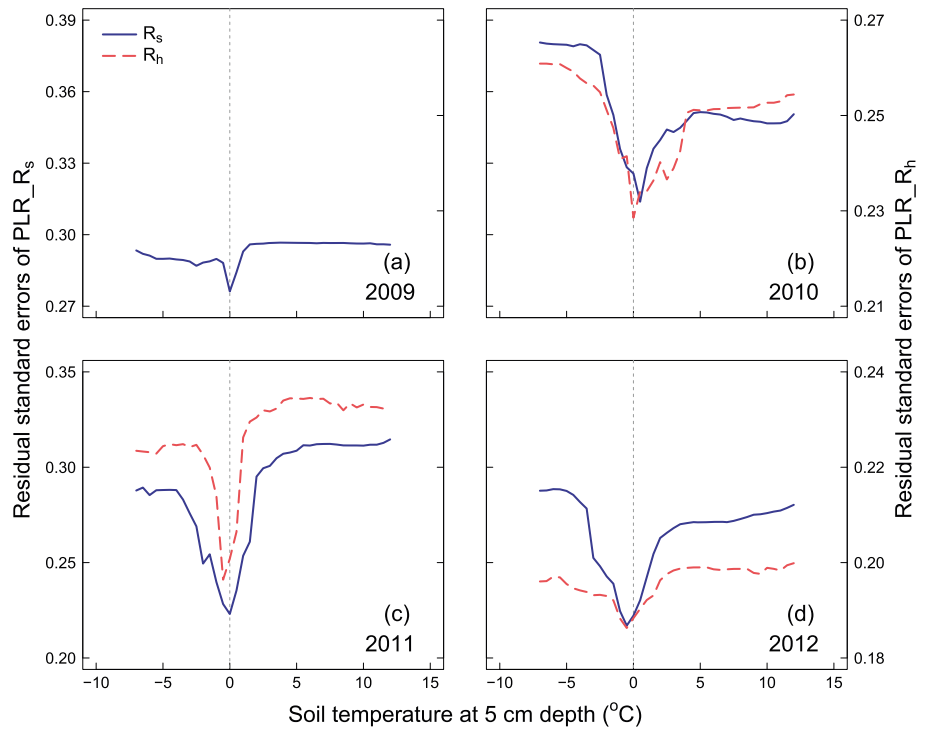


**Figure 4.** Residual standard errors (RSE) of piecewise linear regression model (PLR). Blue (solid) lines represent RSE of PLR model when it was used to analyze the relationship between  $R_s$  and  $ST_5$  (PLR\_ $R_s$ ); red (dashed) lines represent RSE of PLR model when it was used to analyze the relationship between  $R_h$  and  $ST_5$  (PLR\_ $R_h$ ).

chosen as the breakpoint of the  $\ln R_{s,Day}$  versus  $ST_5$  relationship. Further analyses showed that for both  $R_s$  and  $R_h$ , PLR models performed significantly better than OLR models (Table S2).

Therefore, we calculated the  $R_0$  and  $Q_{10}$  of  $R_s$  and  $R_h$  under two different environmental conditions: the non-growing-season frozen soil and the growing-season thawed soil. The ANCOVA showed that in the former, either the  $R_0$  or  $Q_{10}$  of  $R_s$  was not significantly different from their  $R_h$  counterparts ( $P > 0.05$ , Table 5).

**Table 5.** Differences of Reference Respiration Rate ( $R_0$ ) and Temperature Sensitivity ( $Q_{10}$ ) Between the Nongrowing Season and the Growing Season<sup>a</sup>

	2009	2010	2011	2012
<i>Nongrowing season (frozen soil)</i>				
<i>Reference Respiration Rate (<math>R_0</math>, <math>\mu\text{mol CO}_2 \text{ m}^{-2} \text{ s}^{-1}</math>)</i>				
$R_s$	0.46 (0.03) B	0.40 (0.03) aB	0.44 (0.09) aB	0.53 (0.08) aB
$R_h$	—	0.38 (0.02) aB	0.44 (0.02) aB	0.47 (0.03) aB
<i>Temperature Sensitivity (<math>Q_{10}</math>)</i>				
$R_s$	2.89 (0.13) B	2.48 (0.10) aB	2.77 (0.11) aB	2.60 (0.13) aB
$R_h$	—	2.48 (0.06) aB	2.51 (0.17) aB	2.60 (0.16) aB
<i>Growing season (thawed soil)</i>				
<i>Reference Respiration Rate (<math>R_0</math>, <math>\mu\text{mol CO}_2 \text{ m}^{-2} \text{ s}^{-1}</math>)</i>				
$R_s$	0.84 (0.03) A	1.21 (0.03) aA	1.09 (0.02) aA	1.32 (0.05) aA
$R_h$	—	0.73 (0.05) bA	0.75 (0.01) bA	0.69 (0.03) bA
<i>Temperature Sensitivity (<math>Q_{10}</math>)</i>				
$R_s$	5.58 (0.13) A	2.89 (0.10) aA	3.60 (0.12) aA	3.06 (0.13) aA
$R_h$	—	2.77 (0.11) aA	3.28 (0.19) aA	3.08 (0.17) aA

<sup>a</sup>Values in brackets are the standard error of the means ( $n = 3-4$  for  $R_s$  and  $n = 2$  for  $R_h$ ). Letters in lowercase (a and b) within a column indicate a significant difference of  $R_0$  (or  $Q_{10}$ ) between soil respiration ( $R_s$ ) and heterotrophic respiration ( $R_h$ ) in the same season (ANCOVA,  $P < 0.05$ ). Letters in uppercase (A and B) within a column indicate a significant seasonal difference of  $R_0$  (or  $Q_{10}$ ) (ANCOVA,  $P < 0.05$ ).

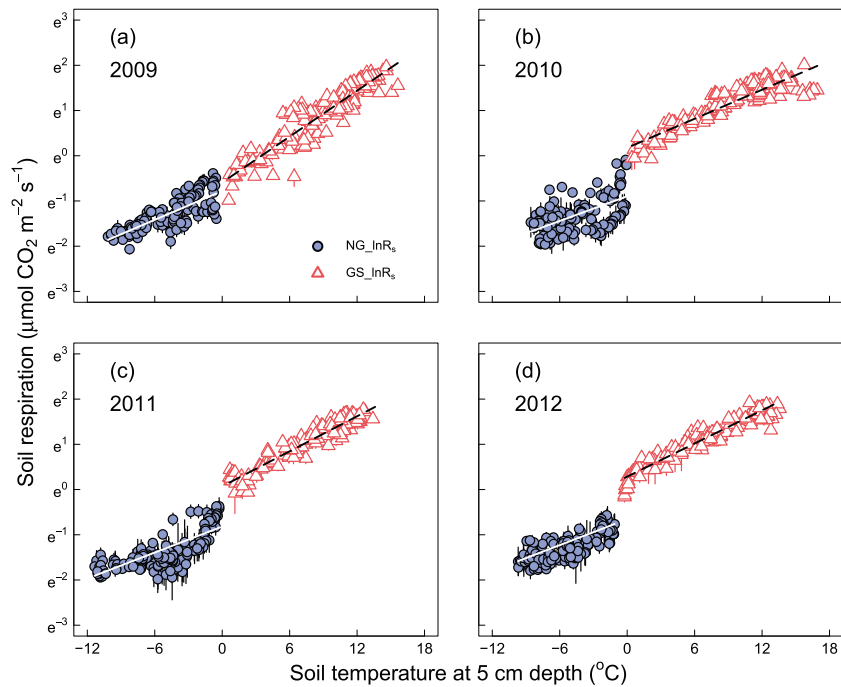


**Figure 5.** Difference of  $R_s$  temperature dependence between the nongrowing season (frozen soil, NG\_ $R_s$ ) and the growing season (thawed soil, GS\_ $R_s$ ). Vertical bars represent the standard error of the means ( $n = 3-4$ ).

In the latter,  $R_s$  and  $R_h$  had a different  $R_0$  ( $P < 0.05$ , Table 5) but a similar  $Q_{10}$  ( $P > 0.05$ , Table 5).  $R_s$  of the non-growing-season frozen soil had lower  $R_0$  and  $Q_{10}$  than that of the growing-season thawed soil ( $P < 0.05$ , Figure 5 and Table 5). Similarly,  $R_h$  of the non-growing-season frozen soil had lower  $R_0$  and  $Q_{10}$  than that of the growing-season thawed soil ( $P < 0.05$ , Table 5). These results indicate that when investigating year-round  $R_s$ , employing two  $Q_{10}$  functions with a breakpoint at 0°C would be better than just using a single  $Q_{10}$  function.

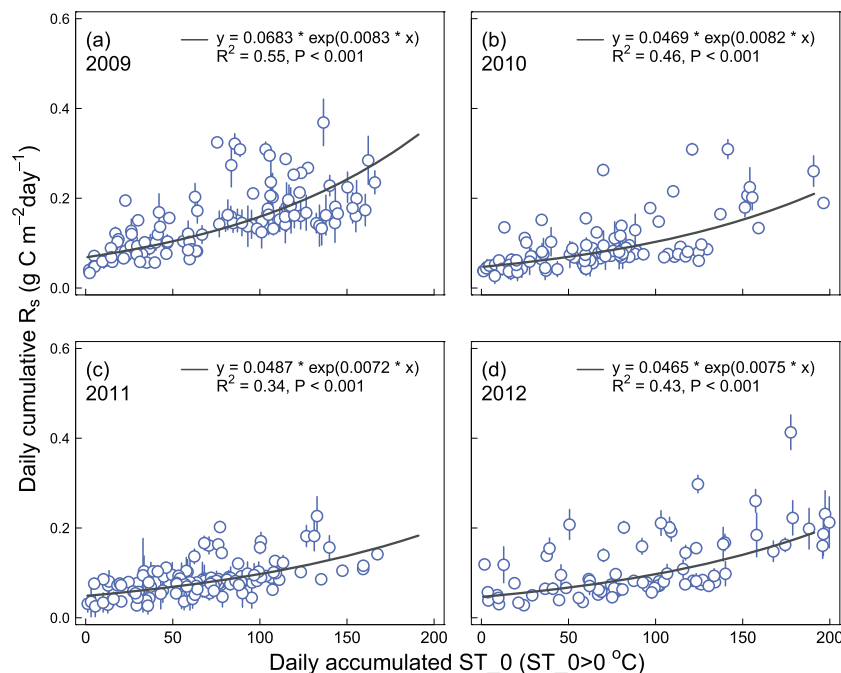


**Figure 6.** (a–d) The relationship between the daily cumulative  $R_s$  and the daily accumulated soil surface temperature ( $ST_0$ ,  $ST_0 > 0^\circ\text{C}$ ) in the nongrowing season. Vertical bars represent the standard error of the means ( $n = 3-4$ ).

### 3.5. Cumulative $R_s$ in the Non-Growing-Season

In the nongrowing season, the daily cumulative  $R_s$  exponentially increased with daily accumulated  $ST_0$  ( $ST_0 > 0^\circ\text{C}$ ), explaining 34–55% of the intraannual variations (Figures 6a–6d). This result is also consistent with our deduction that the surface soil freezing drives the non-growing-season diurnal pattern of  $R_s$ .

## 4. Discussion

The non-growing-season  $R_s$  is an essential carbon cycling process in the Tibetan alpine grassland. The main conclusions of this study are the following: (1) the non-growing-season cumulative  $R_s$  is large, accounting for 11.8–13.2% of the annual total  $R_s$ , indicating that it plays a significant role in the global carbon cycling and (2) surface soil freezing, bulk soil freezing, and accumulated surface soil temperature are the day-, season-, and year-scale drivers of the non-growing-season  $R_s$ , respectively. Our results suggest that warmer winters can trigger carbon loss from the Tibetan alpine grassland because of higher-temperature sensitivity of thawed soils than frozen soils.

### 4.1. General Patterns of the Non-Growing-Season $R_s$

The large amount of carbon respired during the nongrowing season suggests that the non-growing-season  $R_s$  of the Tibetan alpine grassland leads to significant carbon loss and plays an important role in the global carbon cycle.  $R_h$ , stemming from the microbial decomposition of soil organic matter was the dominant component of non-growing-season  $R_s$ ; it accounted for one fifth of the growing-season  $R_h$ . These results imply that in the Tibetan alpine grassland, though there is no persistent snow cover in the nongrowing season and the soil temperature is low, soil microbes are still active and are the major biotic controller of the non-growing-season  $R_s$ . Therefore, the non-growing-season carbon processes must be taken into consideration when assessing the carbon sink/source function of the Tibetan alpine grassland; otherwise, the annual decomposition of soil organic carbon will be significantly underestimated.

The non-growing-season cumulative  $R_s$  ( $82\text{--}89\text{ g C m}^{-2}$ ) and its contribution to annual total  $R_s$  (11.8–13.2%) of the Tibetan alpine grassland are lower than the  $R_s$  values ( $103\text{ to }176\text{ g C m}^{-2}$ ) and annual contributions (14–40%) reported for the heath tundra ecosystems [Elberling, 2007; Larsen et al., 2007; Morgner et al., 2010; Sullivan et al., 2010]. When compared to sedge and tussock tundra, which share many similarities with the Tibetan alpine grassland including the vegetation, the Tibetan alpine grassland has higher non-growing-season cumulative  $R_s$ . On the other hand, the annual contribution of the non-growing-season cumulative  $R_s$  to total  $R_s$  is lower than the reported range (17–30%) of the sedge and tussock tundra [Fahnestock et al., 1999; Morgner et al., 2010; Oechel et al., 1997; Sullivan et al., 2008; Welker et al., 2004]. Variation in estimated non-growing-season cumulative  $R_s$  among ecosystems is likely due to the differences in non-growing-season temperature [Wang et al., 2011], snow cover and its insulating effect [Brooks et al., 1997; Nobrega and Grogan, 2007; Welker et al., 2000], vegetation type [Grogan and Jonasson, 2006], substrate availability [Brooks et al., 2004], grazing intensity [Chen et al., 2013], and  $R_s$  measurement technique [Grogan and Chapin, 1999; McDowell et al., 2000].

The lower annual contribution of non-growing-season cumulative  $R_s$  to total  $R_s$  compared to that of sedge and tussock tundra is likely due to the unique non-growing-season climate of this plateau. More specifically, in the nongrowing season, the Tibetan alpine grassland receives only 6–8% of its annual precipitation and usually has no thick and persistent snowpack. In contrast, in tundra ecosystems, the nongrowing season receives 50–80% of annual precipitation via snowfall, and the non-growing-season snow depth is often  $> 50\text{ cm}$  [Sullivan et al., 2008] or even  $> 100\text{ cm}$  [Brooks et al., 2004; Morgner et al., 2010]. The duration and depth of snow cover can have a marked impact on soil temperature [Campbell et al., 2005], and manipulated deeper snowpack has been shown to induce higher non-growing-season  $R_s$  than ambient plots [Morgner et al., 2010; Nobrega and Grogan, 2007; Schimel et al., 2004].

The relatively short nongrowing season and high growing-season  $R_s$  of the Tibetan alpine grassland than arctic tundra may also lead to lower contribution of the non-growing-season cumulative  $R_s$ . Though the non-growing-season length is  $\sim 180$  days on the Tibetan Plateau, it is relatively shorter than that of the tundra ecosystems which can be  $\sim 240$  days [Belshé et al., 2013; Fahnestock et al., 1999; Grogan and Jonasson, 2006; Oechel et al., 1997]. In addition, the growing-season cumulative  $R_s$  of our study site was as high as  $584\text{--}633\text{ g C m}^{-2}$ , which is 3–8 times higher than that of tundra ecosystems ( $82\text{--}200\text{ g C m}^{-2}$ ) [Elberling, 2007; Grogan and Chapin, 1999]; this explains the lower annual contribution of the non-growing-season  $R_s$  in the Tibetan alpine grassland than the arctic tundra ecosystems.

#### 4.2. The Day-, Season-, and Year-Scale Drivers of the Non-Growing-Season $R_s$

We observed that the non-growing-season  $R_s$  had a lower daily minimum  $R_s$  rate and amplitude and an earlier peak than those of the growing season. Two factors may explain this seasonal variation of diurnal pattern. Autotrophic respiration ( $R_a$ ) of plant roots is the major component of the growing-season  $R_s$  that accounts for 40.4–48.8% of the growing-season  $R_s$ , but it accounts for only 1.9–11.9% of the non-growing-season  $R_s$ . In the nongrowing season, the interruption of the belowground transmission of plant photosynthate lowers  $R_a$  and consequently induces a lower daily minimum  $R_s$  rate and a lower amplitude [Högberg *et al.*, 2001; Kuzyakov, 2006; Tang *et al.*, 2005].

Our study shows that the drivers of diurnal pattern of  $R_s$  are different between the growing and nongrowing seasons. In the growing season, soil temperature (ST\_5) is the most important driver of diurnal pattern of  $R_s$ , while temperature-induced surface soil freezing, a unique characteristic of the non-growing-season soil of this plateau, drives the non-growing-season diurnal pattern of  $R_s$ . Surface soil freezing-thawing process is regulated by the climate properties of the Tibetan Plateau in nongrowing season, i.e., high solar radiation, no polar night, and no thermal insulation of snow cover. In the night, surface soil temperature drops quickly to  $< 0^\circ\text{C}$  due to the heat exchange between soil and atmosphere; in the day, solar radiation warms the surface soil directly and induces thawing of surface soil [Bristow and Campbell, 1984; Pan *et al.*, 2013]. The  $\text{CO}_2$  production continues in frozen soil at night because soil microbes can maintain their activities at extremely low temperature [Panikov *et al.*, 2006], but the  $\text{CO}_2$  produced is trapped by frozen ground [Elberling and Brandt, 2003]. In the day, rising temperatures and thawing of surface soil allow  $\text{CO}_2$  to be released, inducing a pulse in  $\text{CO}_2$  emission [Matzner and Borken, 2008]. Because surface soil temperature rises faster than the soil temperature at 5 cm depth during the daytime, this results in an earlier peak time than that of the growing season.

Bulk soil freezing is an important regulator of the season-scale variation in temperature dependence of  $R_s$ , and both the  $R_0$  and  $Q_{10}$  of the non-growing-season  $R_s$  were lower than their growing-season counterparts. The relatively lower  $Q_{10}$  in the nongrowing season is not consistent with a previous study conducted in a seasonal snow-covered alpine coniferous forest in Rocky Mountains, USA. In that study, the maximum snow depth was  $\sim 120$  cm and the  $R_s$  showed a significantly higher  $Q_{10}$  under snowpack due to soil microbial communities of fast substrate utilization [Monson *et al.*, 2006b]. Thin and patchy snow cover in the Tibetan Plateau and differences in soil water content may explain these apparent inconsistencies. More specifically, under thin snow cover, soil microbes had a lower activity than under thick snow cover, due to the absence of insulation effects [Brooks *et al.*, 1998; Brooks and Williams, 1999]. In addition, in a laboratory soil incubation study,  $Q_{10}$  increased with higher soil water content when soil temperature was  $< 0^\circ\text{C}$  [Elberling and Brandt, 2003]. Thus, the low precipitation and drought during the nongrowing season in the Tibetan alpine grassland may explain the lower non-growing-season  $Q_{10}$  than the seasonal snow-covered ecosystems. On the other hand, not considering the breakpoint of the functional relationship between  $R_s$  and soil temperature may account for the inconsistent reports. When the changes of  $R_0$  around the breakpoint are not included in models, it may lead to overestimation of the non-growing-season  $Q_{10}$ .

Our study shows that using two  $Q_{10}$  functions with a breakpoint of  $0^\circ\text{C}$  is superior to using a single  $Q_{10}$  function when investigating year-round temperature dependence of  $R_s$  (or  $R_h$ ), but the  $Q_{10}$  function employed in current analyses cannot mechanistically explain why  $R_0$  and  $Q_{10}$  vary between seasons and why an observed breakpoint exists. Here we emphasize the effects of bulk soil freezing on unfrozen water content and substrate supply for soil microorganisms. In a field study, it was shown that fluid water is depleted when soil water freezes under temperature lower than  $0^\circ\text{C}$ ; unfrozen water content exponentially decreases with soil temperature when soil temperature is  $< 0^\circ\text{C}$  [Schimel *et al.*, 2006]. Recently, another study showed that in frozen soil, unfrozen water content was highly dependent on temperature, especially between  $-2$  and  $0^\circ\text{C}$ , and strongly affects substrate supply, soil microbial activity, and temperature dependence of the non-growing-season  $R_s$  [Tucker, 2014]. Laboratory soil incubation studies have shown that the soil  $\text{CO}_2$  production was negatively correlated with unfrozen water content at  $-4^\circ\text{C}$  [Öquist *et al.*, 2009] and the temperature dependence of  $R_h$  at subzero temperature was moderated by unfrozen water content [Tilston *et al.*, 2010], indicating that soil microbial activity in frozen soil is controlled by water availability. In addition, extremely cold temperature will limit the substrate supply for soil microorganisms. The non-growing-season  $R_s$  is almost entirely from microbial decomposition, which is a temperature-dependent biological process. In this process, activation energy is

one of the dominant abiotic factors according to the Arrhenius kinetic theory, while activation energy is directly related to the molecular structure of substrates. Less reactive and more recalcitrant substrates, which are complex molecules and have higher activation energy, should have higher-temperature sensitivity than the labile substrates [Davidson and Janssens, 2006]. Under freezing temperature, decomposition of recalcitrant substrates is limited due to low activation energy supply, resulting in lower  $R_0$  and  $Q_{10}$  in the nongrowing season. Therefore, a single  $Q_{10}$  model cannot adequately represent the year-round temperature dependence of  $R_s$ .

In the current study, we found that the amount of soil organic carbon decomposed during the nongrowing season contributed a considerable proportion (about one fifth of that in the growing season), which are directly driven by surface soil temperature. Considering that the Tibetan Plateau has been experiencing a larger-than-average trend of warming and the cold months have been facing even faster rate of warming than the growing season during the last decades [Piao *et al.*, 2010; You *et al.*, 2010; Zhang *et al.*, 2013], our study suggests that the warming climate will cause an increase in the non-growing-season soil  $\text{CO}_2$  emission.

### 4.3. Implications

The Tibetan Plateau is one of the most sensitive and vulnerable regions to global warming; it has the largest permafrost coverage in the low-middle latitudes, but the speed of permafrost loss over this plateau has been rapid in the last decades [Cheng, 2005; Cheng and Wu, 2007; Nan *et al.*, 2005; Wu and Zhang, 2010]. Recent studies reported that the permafrost soils may positively feedback to climate warming, because of the increased decomposition rates of soil carbon with rising temperature [Belshé *et al.*, 2013; Dörfer *et al.*, 2013; Koven *et al.*, 2011]. In our study, both  $R_0$  and  $Q_{10}$  of thawed soil were higher than those of the frozen soil, and the thawed soil had the potential to release significantly more  $\text{CO}_2$  into the atmosphere than the frozen soil (Table S3 and Figure S4). Although our study site does not contain permafrost, these results are relevant to permafrost thawing because this site is located in the transitional zone from permafrost to seasonally frozen soil in the northeastern region of the Tibetan Plateau (Figure S5). Considering that this plateau acts as carbon sink [Kato *et al.*, 2006; Zhao *et al.*, 2006], our results suggest that degradation of permafrost area can trigger carbon loss from this plateau, weaken the carbon sink function, or even shift the Tibetan alpine grassland from a net carbon sink to a source.

### Acknowledgments

The authors would like to thank Ben Bond-Lamberty, Eric Davidson, and two anonymous reviewers for their constructive comments and suggestions. We also thank Jacob Weiner and Dan Flynn for their comments and Shaopeng Wang, Yue Shi, and Yinlei Ma for data analysis and interpretation. Yonghui Wang and Huiying Liu made equal contribution to this paper. This study was supported by the National Basic Research Program of China (grants 2010CB950602 and 2014CB954004), National Natural Science Foundation of China (grants 31025005 and 31321061), Strategic Priority Research Program (B) of the Chinese Academy of Sciences (XDA05050404 and XDB03030403), and Chinese Academy of Sciences Research grant (KZCX2-YW-JC404). Haegun Chung is partly supported by the Research Fellowship for International Young Scientists of Chinese Academy of Sciences.

### References

- Belshé, E. F., E. A. G. Schuur, and B. M. Bolker (2013), Tundra ecosystems observed to be  $\text{CO}_2$  sources due to differential amplification of the carbon cycle, *Ecol. Lett.*, doi:10.1111/ele.12164.
- Bergeron, O., H. A. Margolis, T. A. Black, C. Coursolle, A. L. Dunn, A. G. Barr, and S. C. Wofsy (2007), Comparison of carbon dioxide fluxes over three boreal black spruce forests in Canada, *Global Change Biol.*, 13(1), 89–107, doi:10.1111/j.1365-2486.2006.01281.x.
- Bristow, K. L., and G. S. Campbell (1984), On the relationship between incoming solar radiation and daily maximum and minimum temperature, *Agric. For. Meteorol.*, 31(2), 159–166, doi:10.1016/0168-1923(84)90017-0.
- Brooks, P. D., and M. W. Williams (1999), Snowpack controls on nitrogen cycling and export in seasonally snow-covered catchments, *Hydrol. Processes*, 13(14–15), 2177–2190, doi:10.1002/(SICI)1099-1085(199910)13:14/15<2177::AID-HYP850>3.0.CO;2-V.
- Brooks, P. D., S. K. Schmidt, and M. W. Williams (1997), Winter production of  $\text{CO}_2$  and  $\text{N}_2\text{O}$  from Alpine tundra: Environmental controls and relationship to inter-system C and N fluxes, *Oecologia*, 110(3), 403–413, doi:10.1007/PL00008814.
- Brooks, P. D., M. W. Williams, and S. K. Schmidt (1998), Inorganic nitrogen and microbial biomass dynamics before and during spring snowmelt, *Biogeochemistry*, 43(1), 1–15, doi:10.1023/a:1005947511910.
- Brooks, P. D., D. McKnight, and K. Elder (2004), Carbon limitation of soil respiration under winter snowpacks: Potential feedbacks between growing season and winter carbon fluxes, *Global Change Biol.*, 11(2), 231–238, doi:10.1111/j.1365-2486.2004.00877.x.
- Campbell, J. L., M. J. Mitchell, P. M. Groffman, L. M. Christenson, and J. P. Hardy (2005), Winter in northeastern North America: A critical period for ecological processes, *Front. Ecol. Environ.*, 3(6), 314–322, doi:10.1890/1540-9295(2005)003[0314:WINNAA]2.0.CO;2.
- Cao, G. M., Y. H. Tang, W. H. Mo, Y. A. Wang, Y. N. Li, and X. Q. Zhao (2004), Grazing intensity alters soil respiration in an alpine meadow on the Tibetan Plateau, *Soil Biol. Biochem.*, 36(2), 237–243, doi:10.1016/j.soilbio.2003.09.010.
- Chen, W., *et al.* (2013), Carbon dioxide emission from temperate semiarid steppe during the non-growing season, *Atmos. Environ.*, 64(0), 141–149, doi:10.1016/j.atmosenv.2012.10.004.
- Cheng, G. (2005), Permafrost studies in the Qinghai-Tibet Plateau for road construction, *J. Cold Reg. Eng.*, 19(1), 19–29, doi:10.1061/(ASCE)0887-381X(2005)19:1(19).
- Cheng, G., and T. Wu (2007), Responses of permafrost to climate change and their environmental significance, Qinghai-Tibet Plateau, *J. Geophys. Res.*, 112, F02S03, doi:10.1029/2006JF000631.
- Chinese Soil Taxonomy Research Group (1995), *Chinese Soil Taxonomy*, pp. 58–147, Science Press, Beijing, China.
- Davidson, E. A., and I. A. Janssens (2006), Temperature sensitivity of soil carbon decomposition and feedbacks to climate change, *Nature*, 440(7081), 165–173, doi:10.1038/nature04514.
- Dörfer, C., P. Kühn, F. Baumann, J. S. He, and T. Scholten (2013), Soil organic carbon pools and stocks in permafrost-affected soils on the Tibetan Plateau, *PLoS One*, 8(2), e57024, doi:10.1371/journal.pone.0057024.
- Elberling, B. (2007), Annual soil  $\text{CO}_2$  effluxes in the High Arctic: The role of snow thickness and vegetation type, *Soil Biol. Biochem.*, 39(2), 646–654, doi:10.1016/j.soilbio.2006.09.017.
- Elberling, B., and K. K. Brandt (2003), Uncoupling of microbial  $\text{CO}_2$  production and release in frozen soil and its implications for field studies of arctic C cycling, *Soil Biol. Biochem.*, 35(2), 263–272, doi:10.1016/S0038-0717(02)00258-4.

- Fahnestock, J. T., M. H. Jones, P. D. Brooks, D. A. Walker, and J. M. Welker (1998), Winter and early spring CO<sub>2</sub> efflux from tundra communities of northern Alaska, *J. Geophys. Res.*, *103*(D22), 29,023–29,027, doi:10.1029/98JD00805.
- Fahnestock, J. T., M. H. Jones, and J. M. Welker (1999), Wintertime CO<sub>2</sub> efflux from arctic soils: Implications for annual carbon budgets, *Global Biogeochem. Cycles*, *13*(3), 775–779, doi:10.1029/1999GB900006.
- Geng, Y., et al. (2012), Soil respiration in Tibetan alpine grasslands: Belowground biomass and soil moisture, but not soil temperature, best explain the large-scale patterns, *PLoS One*, *7*(4), e34968, doi:10.1371/journal.pone.0034968.
- Grogan, P., and F. S. Chapin (1999), Arctic soil respiration: Effects of climate and vegetation depend on season, *Ecosystems*, *2*(5), 451–459, doi:10.1007/s100219900093.
- Grogan, P., and S. Jonasson (2006), Ecosystem CO<sub>2</sub> production during winter in a Swedish subarctic region: The relative importance of climate and vegetation type, *Global Change Biol.*, *12*(8), 1479–1495, doi:10.1111/j.1365-2486.2006.01184.x.
- Guo, D. L., M. X. Yang, and H. J. Wang (2011), Characteristics of land surface heat and water exchange under different soil freeze/thaw conditions over the central Tibetan Plateau, *Hydrol. Processes*, *25*(16), 2531–2541, doi:10.1002/hyp.8025.
- Högberg, P., et al. (2001), Large-scale forest girdling shows that current photosynthesis drives soil respiration, *Nature*, *411*(6839), 789–792, doi:10.1038/35081058.
- Jing, X., Y. Wang, H. Chung, Z. Mi, S. Wang, H. Zeng, and J.-S. He (2013), No temperature acclimation of soil extracellular enzymes to experimental warming in an alpine grassland ecosystem on the Tibetan Plateau, *Biogeochemistry*, *117*(1), 39–54, doi:10.1007/s10533-013-9844-2.
- Kato, T., et al. (2004), Seasonal patterns of gross primary production and ecosystem respiration in an alpine meadow ecosystem on the Qinghai-Tibetan Plateau, *J. Geophys. Res.*, *109*, D12109, doi:10.1029/2003JD003951.
- Kato, T., Y. H. Tang, S. Gu, M. Hirota, M. Y. Du, Y. N. Li, and X. Q. Zhao (2006), Temperature and biomass influences on interannual changes in CO<sub>2</sub> exchange in an alpine meadow on the Qinghai-Tibetan Plateau, *Global Change Biol.*, *12*(7), 1285–1298, doi:10.1111/j.1365-2486.2006.01153.x.
- Kimball, B. A., M. M. Conley, S. Wang, X. Lin, C. Luo, J. Morgan, and D. Smith (2008), Infrared heater arrays for warming ecosystem field plots, *Global Change Biol.*, *14*(2), 309–320, doi:10.1111/j.1365-2486.2007.01486.x.
- Konestabo, H. S., A. Michelsen, and M. Holmström (2007), Responses of springtail and mite populations to prolonged periods of soil freeze-thaw cycles in a sub-arctic ecosystem, *Appl. Soil Ecol.*, *36*(2–3), 136–146, doi:10.1016/j.apsoil.2007.01.003.
- Körner, C., and J. Paulsen (2004), A world-wide study of high altitude treeline temperatures, *J. Biogeogr.*, *31*(5), 713–732, doi:10.1111/j.1365-2699.2003.01043.x.
- Koven, C. D., et al. (2011), Permafrost carbon-climate feedbacks accelerate global warming, *Proc. Natl. Acad. Sci. U.S.A.*, *108*(36), 14,769–14,774, doi:10.1073/pnas.1103910108.
- Kuz'yakov, Y. (2006), Sources of CO<sub>2</sub> efflux from soil and review of partitioning methods, *Soil Biol. Biochem.*, *38*(3), 425–448, doi:10.1016/j.soilbio.2005.08.020.
- Larsen, K. S., P. Grogan, S. Jonasson, and A. Michelsen (2007), Respiration and microbial dynamics in two subarctic ecosystems during winter and spring thaw: Effects of increased snow depth, *Arctic, Antarctic, Alpine Res.*, *39*(2), 268–276, doi:10.1657/1523-0430(2007)39[268:RAMDIT]2.0.CO;2.
- Liptzin, D., M. W. Williams, D. Helmig, B. Seok, G. Filippa, K. Chowanski, and J. Hueber (2009), Process-level controls on CO<sub>2</sub> fluxes from a seasonally snow-covered subalpine meadow soil, Niwot Ridge, Colorado, *Biogeochemistry*, *95*(1), 151–166, doi:10.1007/s10533-009-9303-2.
- Luo, C. Y., et al. (2010), Effect of warming and grazing on litter mass loss and temperature sensitivity of litter and dung mass loss on the Tibetan Plateau, *Global Change Biol.*, *16*(5), 1606–1617, doi:10.1111/j.1365-2486.2009.02026.x.
- Mariko, S., N. Nishimura, W. H. Mo, Y. Matsui, T. Kibe, and H. Koizumi (2000), Winter CO<sub>2</sub> flux from soil and snow surfaces in a cool-temperate deciduous forest, Japan, *Ecol. Res.*, *15*(4), 363–372, doi:10.1046/j.1440-1703.2000.00357.x.
- Matzner, E., and W. Borken (2008), Do freeze-thaw events enhance C and N losses from soils of different ecosystems? A review, *Eur. J. Soil Sci.*, *59*(2), 274–284, doi:10.1111/j.1365-2389.2007.00992.x.
- McDowell, N. G., J. D. Marshall, T. D. Hooker, and R. Musselman (2000), Estimating CO<sub>2</sub> flux from snowpacks at three sites in the Rocky Mountains, *Tree Physiol.*, *20*(11), 745–753, doi:10.1093/treephys/20.11.745.
- McGuire, A. D., et al. (2009), Sensitivity of the carbon cycle in the Arctic to climate change, *Ecol. Monogr.*, *79*(4), 523–555, doi:10.1890/08-2025.1.
- McMahon, S. K., M. D. Wallenstein, and J. P. Schimel (2011), A cross-seasonal comparison of active and total bacterial community composition in Arctic tundra soil using bromodeoxyuridine labeling, *Soil Biol. Biochem.*, *43*(2), 287–295, doi:10.1016/j.soilbio.2010.10.013.
- Mikan, C. J., J. P. Schimel, and A. P. Doyle (2002), Temperature controls of microbial respiration in arctic tundra soils above and below freezing, *Soil Biol. Biochem.*, *34*(11), 1785–1795, doi:10.1016/S0038-0717(02)00168-2.
- Mo, W., M. S. Lee, M. Uchida, M. Inatomi, N. Saigusa, S. Mariko, and H. Koizumi (2005), Seasonal and annual variations in soil respiration in a cool-temperate deciduous broad-leaved forest in Japan, *Agric. For. Meteorol.*, *134*(1–4), 81–94, doi:10.1016/j.agrformet.2005.08.015.
- Monson, R. K., S. P. Burns, M. W. Williams, A. C. Delany, M. Weintraub, and D. A. Lipson (2006a), The contribution of beneath-snow soil respiration to total ecosystem respiration in a high-elevation, subalpine forest, *Global Biogeochem. Cycles*, *20*, GB3030, doi:10.1029/2005GB002684.
- Monson, R. K., D. L. Lipson, S. P. Burns, A. A. Turnipseed, A. C. Delany, M. W. Williams, and S. K. Schmidt (2006b), Winter forest soil respiration controlled by climate and microbial community composition, *Nature*, *439*(7077), 711–714, doi:10.1038/nature04555.
- Morgner, E., B. Elberling, D. Stöbel, and E. J. Cooper (2010), The importance of winter in annual ecosystem respiration in the High Arctic: Effects of snow depth in two vegetation types, *Polar Res.*, *29*(1), 58–74, doi:10.1111/j.1751-8369.2010.00151.x.
- Nan, Z. T., S. X. Li, and G. D. Cheng (2005), Prediction of permafrost distribution on the Qinghai-Tibet Plateau in the next 50 and 100 years, *Sci. China Ser. D*, *48*(6), 797–804, doi:10.1360/03yd0258.
- Nobrega, S., and P. Grogan (2007), Deeper snow enhances winter respiration from both plant-associated and bulk soil carbon pools in Birch Hummock tundra, *Ecosystems*, *10*(3), 419–431, doi:10.1007/s10021-007-9033-z.
- Oechel, W. C., G. Vourlitis, and S. J. Hastings (1997), Cold season CO<sub>2</sub> emission from arctic soils, *Global Biogeochem. Cycles*, *11*(2), 163–172, doi:10.1029/96GB03035.
- Öquist, M. G., T. Sparman, L. Klemetsson, S. H. Drotz, H. Grip, J. Schleucher, and M. Nilsson (2009), Water availability controls microbial temperature responses in frozen soil CO<sub>2</sub> production, *Global Change Biol.*, *15*(11), 2715–2722, doi:10.1111/j.1365-2486.2009.01898.x.
- Pan, T., S. H. Wu, E. F. Dai, and Y. J. Liu (2013), Estimating the daily global solar radiation spatial distribution from diurnal temperature ranges over the Tibetan Plateau in China, *Appl. Energy*, *107*, 384–393, doi:10.1016/j.apenergy.2013.02.053.
- Panikov, N. S., P. W. Flanagan, W. C. Oechel, M. A. Mastepanov, and T. R. Christensen (2006), Microbial activity in soils frozen to below –39 °C, *Soil Biol. Biochem.*, *38*(12), 785–794, doi:10.1016/j.soilbio.2005.07.004.
- Piao, S. L., P. Friedlingstein, P. Ciais, N. Viovy, and J. Demarty (2007), Growing season extension and its impact on terrestrial carbon cycle in the Northern Hemisphere over the past 2 decades, *Global Biogeochem. Cycles*, *21*, GB3018, doi:10.1029/2006GB002888.
- Piao, S. L., et al. (2010), The impacts of climate change on water resources and agriculture in China, *Nature*, *467*(7311), 43–51, doi:10.1038/nature09364.
- R Core Team (2012), *R: A Language and Environment for Statistical Computing*, R Foundation for Statistical Computing, Vienna, Austria.

- Schimel, J. P., C. Bilbrough, and J. M. Welker (2004), Increased snow depth affects microbial activity and nitrogen mineralization in two Arctic tundra communities, *Soil Biol. Biochem.*, *36*(2), 217–227, doi:10.1016/j.soilbio.2003.09.008.
- Schimel, J. P., J. Fahnestock, G. Michaelson, C. Mikan, C. L. Ping, V. E. Romanovsky, and J. Welker (2006), Cold-season production of CO<sub>2</sub> in arctic soils: Can laboratory and field estimates be reconciled through a simple modeling approach?, *Arctic Antarctic Alpine Res.*, *38*(2), 249–256, doi:10.1657/1523-0430(2006)38[249:CPOCIA]2.0.CO;2.
- Seok, B., D. Helmig, M. Williams, D. Liptzin, K. Chowanski, and J. Hueber (2009), An automated system for continuous measurements of trace gas fluxes through snow: An evaluation of the gas diffusion method at a subalpine forest site, Niwot Ridge, Colorado, *Biogeochemistry*, *95*(1), 95–113, doi:10.1007/s10533-009-9302-3.
- Shi, P. L., X. Z. Zhang, Z. M. Zhong, and H. Ouyang (2006), Diurnal and seasonal variability of soil CO<sub>2</sub> efflux in a cropland ecosystem on the Tibetan Plateau, *Agric. For. Meteorol.*, *137*(3–4), 220–233, doi:10.1016/j.agrformet.2006.02.008.
- Shi, Y., F. Baumann, Y. Ma, C. Song, P. Kühn, T. Scholten, and J. S. He (2012), Organic and inorganic carbon in the topsoil of the Mongolian and Tibetan grasslands: Pattern, control and implications, *Biogeosciences*, *9*(6), 2287–2299, doi:10.5194/bg-9-1869-2012.
- Sullivan, P. F., J. M. Welker, S. J. T. Arens, and B. Sveinbjörnsson (2008), Continuous estimates of CO<sub>2</sub> efflux from arctic and boreal soils during the snow-covered season in Alaska, *J. Geophys. Res.*, *113*, G04009, doi:10.1029/2008JG000715.
- Sullivan, P. F., S. J. T. Arens, B. Sveinbjörnsson, and J. M. Welker (2010), Modeling the seasonality of belowground respiration along an elevation gradient in the western Chugach Mountains, Alaska, *Biogeochemistry*, *101*(1–3), 61–75, doi:10.1007/s10533-010-9471-0.
- Tan, K., et al. (2010), Application of the ORCHIDEE global vegetation model to evaluate biomass and soil carbon stocks of Qinghai-Tibetan grasslands, *Global Biogeochem. Cycles*, *24*, GB1013, doi:10.1029/2009GB003530.
- Tang, J., D. D. Baldocchi, and L. Xu (2005), Tree photosynthesis modulates soil respiration on a diurnal time scale, *Global Change Biol.*, *11*(8), 1298–1304, doi:10.1111/j.1365-2486.2005.00978.x.
- Tang, M., and E. R. Reiter (1984), Plateau monsoons of the Northern Hemisphere: A comparison between North America and Tibet, *Mon. Weather Rev.*, *112*(4), 617–637, doi:10.1175/1520-0493(1984)112<0617:PMOTNH>2.0.CO;2.
- Tanja, S., et al. (2003), Air temperature triggers the recovery of evergreen boreal forest photosynthesis in spring, *Global Change Biol.*, *9*(10), 1410–1426, doi:10.1046/j.1365-2486.2003.00597.x.
- Tian, L., et al. (2003), Oxygen-18 concentrations in recent precipitation and ice cores on the Tibetan Plateau, *J. Geophys. Res.*, *108*(D9), 4293, doi:10.1029/2002JD002173.
- Tilston, E. L., T. Sparrman, and M. G. Öquist (2010), Unfrozen water content moderates temperature dependence of sub-zero microbial respiration, *Soil Biol. Biochem.*, *42*(9), 1396–1407, doi:10.1016/j.soilbio.2010.04.018.
- Toms, J. D., and M. L. Lesperance (2003), Piecewise regression: A tool for indentifying ecological thresholds, *Ecology*, *84*(8), 2034–2041, doi:10.1890/02-0472.
- Tucker, C. (2014), Reduction of air- and liquid water-filled soil pore space with freezing explains high temperature sensitivity of soil respiration below 0°C, *Soil Biol. Biochem.*, *78*, 90–96, doi:10.1016/j.soilbio.2014.06.018.
- Wang, S. P., et al. (2012), Effects of warming and grazing on soil N availability, species composition, and ANPP in an alpine meadow, *Ecology*, *93*(11), 2365–2376, doi:10.1890/11-1408.1.
- Wang, T., et al. (2011), Controls on winter ecosystem respiration in temperate and boreal ecosystems, *Biogeosciences*, *8*(7), 2009–2025, doi:10.5194/bg-8-2009-2011.
- Welker, J. M., J. T. Fahnestock, and M. H. Jones (2000), Annual CO<sub>2</sub> flux in dry and moist arctic tundra: Field responses to increases in summer temperatures and winter snow depth, *Clim. Change*, *44*(1–2), 139–150, doi:10.1023/A:100555012742.
- Welker, J. M., J. T. Fahnestock, G. H. R. Henry, K. W. O’Dea, and R. A. Chimner (2004), CO<sub>2</sub> exchange in three Canadian High Arctic ecosystems: Response to long-term experimental warming, *Global Change Biol.*, *10*(12), 1981–1995, doi:10.1111/j.1365-2486.2004.00857.x.
- Wu, Q. B., and T. J. Zhang (2010), Changes in active layer thickness over the Qinghai-Tibetan Plateau from 1995 to 2007, *J. Geophys. Res.*, *115*, D09107, doi:10.1029/2009JD012974.
- Xu, Z. F., C. A. Wan, P. Xiong, Z. Tang, R. Hu, G. Cao, and Q. Liu (2010), Initial responses of soil CO<sub>2</sub> efflux and C, N pools to experimental warming in two contrasting forest ecosystems, Eastern Tibetan Plateau, China, *Plant Soil*, *336*(1–2), 183–195, doi:10.1007/s11104-010-0461-8.
- Yang, Y. H., J. Y. Fang, Y. H. Tang, C. J. Ji, C. Y. Zheng, J. S. He, and B. A. Zhu (2008), Storage, patterns and controls of soil organic carbon in the Tibetan grasslands, *Global Change Biol.*, *14*(7), 1592–1599, doi:10.1111/j.1365-2486.2008.01591.x.
- You, Q., S. Kang, N. Pepin, W.-A. Flügel, A. Sanchez-Lorenzo, Y. Yan, and Y. Zhang (2010), Climate warming and associated changes in atmospheric circulation in the eastern and central Tibetan Plateau from a homogenized dataset, *Global Planet. Change*, *72*(1–2), 11–24, doi:10.1016/j.gloplacha.2010.04.003.
- Zhang, G. L., Y. J. Zhang, J. W. Dong, and X. M. Xiao (2013), Green-up dates in the Tibetan Plateau have continuously advanced from 1982 to 2011, *Proc. Natl. Acad. Sci. U.S.A.*, *110*(11), 171–176, doi:10.1073/pnas.1210423110.
- Zhang, X. P., Y. F. Shi, and T. D. Yao (1995), Variational features of precipitation δ<sup>18</sup>O in Northeast Qinghai-Tibet Plateau, *Sci. China Ser. B*, *38*(7), 854–864.
- Zhao, L., Y. N. Li, S. X. Xu, H. K. Zhou, S. Gu, G. R. Yu, and X. Q. Zhao (2006), Diurnal, seasonal and annual variation in net ecosystem CO<sub>2</sub> exchange of an alpine shrubland on Qinghai-Tibetan plateau, *Global Change Biol.*, *12*(10), 1940–1953, doi:10.1111/j.1365-2486.2006.01197.x.
- Zhao, X. Q., and X. M. Zhou (1999), Ecological basis of alpine meadow ecosystem management in Tibet: Haibei alpine meadow ecosystem research station, *Ambio*, *28*(8), 642–647.
- Zhu, J. X., X. H. He, F. Z. Wu, W. Q. Yang, and B. Tan (2012), Decomposition of *Abies faxoniana* litter varies with freeze-thaw stages and altitudes in subalpine/alpine forests of southwest China, *Scand. J. For. Res.*, *27*(6), 586–596, doi:10.1080/02827581.2012.670726.
- Zimov, S. A., S. P. Davidov, Y. V. Voropaev, S. F. Prosiannikov, I. P. Semiletov, M. C. Chapin, and F. S. Chapin (1996), Siberian CO<sub>2</sub> efflux in winter as a CO<sub>2</sub> source and cause of seasonality in atmospheric CO<sub>2</sub>, *Clim. Change*, *33*(1), 111–120, doi:10.1007/BF00140516.